

Microstructure evolution and phase composition of high-manganese austenitic steels

L.A. Dobrzański^a, A. Grajcar^{b,*}, W. Borek^a

^a Division of Materials Processing Technology, Management and Computer Techniques in Materials Science, Institute of Engineering Materials and Biomaterials, Silesian University of Technology, ul. Konarskiego 18a, 44-100 Gliwice, Poland

^b Division of Constructional and Special Materials, Institute of Engineering Materials and Biomaterials, Silesian University of Technology, ul. Konarskiego 18a, 44-100 Gliwice, Poland

* Corresponding author: E-mail address: adam.grajcar@polsl.pl

Received 23.09.2008; published in revised form 01.12.2008

Materials

ABSTRACT

Purpose: The aim of the paper is to determine the influence of hot-working conditions on microstructure evolution and phase composition of new-developed high-manganese austenitic steels.

Design/methodology/approach: Determination of processes controlling strain hardening was carried out in continuous compression test using Gleeble 3800 thermo-mechanical simulator. Evaluation of processes controlling work hardening and occurring after deformation at 900°C were identified by microstructure observations of the specimens solution heat-treated after plastic deformation to a true strain equal 0.23, 0.50 and 0.91. Phase composition of steels was confirmed by X-ray diffraction analysis.

Findings: The steels have a fine-grained austenite microstructure with many annealing twins to a temperature of about 1000°C. The initiation of dynamic recrystallization occurs already after true deformation equal 0.29. Participation of fine grains arranged in a matrix of dynamically recovered grains essentially increases after increasing true strain to 0.5. Fully dynamically recrystallized microstructure of steel can be obtained after the true strain equal 0.9. The conditions of hot-working influence phase state of investigated steels. Steel no. 1 keeps stable austenite microstructure independently from conditions of plastic deformation. Steel with initial bi-phase microstructure keeps a certain portion of ϵ martensite, yet dependant on conditions of hot-working.

Research limitations/implications: To determine in detail the hot-working behaviour of developed steels, a progress of microstructure evolution in subsequent stages of multi-stage compression test should be investigated.

Practical implications: The obtained microstructure – hot-working conditions relationships and stress-strain curves can be useful in determination of power-force parameters of hot-rolling for sheets with fine-grained austenitic structures.

Originality/value: The hot-working behaviour and microstructure evolution in various conditions of plastic deformation for new-developed high-manganese austenitic steels with Nb and Ti microadditions were investigated.

Keywords: Metallic alloys; High-manganese steels; Hot-working; Dynamic recrystallization; Metadynamic recrystallization

1. Introduction

Automotive industry is one of the most dynamically developing branches of the global market. Strong competition in the field of automotive market and expansion of new materials with low density, based on aluminium, magnesium as well as polymer composite materials, in last twenty years have led to great activity of steel concerns which had to meet the challenges of the beginning of XXI century. A new look at the role of individual elements generally used for steels and the possibility of new metallurgical technologies application have led to development of steels with a wide range of mechanical properties and formability used in automotive industry. These are IF- (Interstitial Free), BH- (Bake Hardening), IS- (Isotropic DP- (Dual Phase), TRIP- (Transformation Induced Plasticity), CP- (Complex Phase) and TMS- (Martensitic) steels [1-5].

New possibilities appeared at the beginning of this century, when the effect of strain-induced martensitic transformation of γ phase was attempted to be applied in austenitic steels. This effect was used many years ago but for expensive Cr-Ni steels [6]. Nowadays, new group of high-manganese austenitic steels with variable concentration of Mn, Al and Si was proposed showing high potential for their application in automotive industry. These steels meet the needs of automotive industry in a very wide range, concerning optimization of vehicles' mass and fuel consumption, safety of passengers, corrosion resistance and limiting the pollution of environment caused by motorization [7].

In case of manganese concentration below 25% it's possible to use TRIP effect (Transformation Induced Plasticity) consisting in steel hardening in the consequence of $\gamma_{A1} \rightarrow \epsilon_{A3}$ or $\gamma_{A1} \rightarrow \epsilon_{A3} \rightarrow \alpha'_{A2}$ martensitic transformation occurring during cold forming [8]. Martensite ϵ with A3 hexagonal lattice is formed during plastic strain only when stacking fault energy SFE of austenite is lower than 20 mJ/m^2 [9, 10]. Addition of aluminium into steel increases SFE and austenite stability which leads to suppressed influence on martensitic transformation. While the addition of silicon decreases SFE and allows occurring of $\gamma \rightarrow \epsilon$ transformation. In case when manganese concentration in the steel exceeds 25%, the stability of austenite during plastic strain is maintained enhancing mechanical properties due to mechanical twinning – TWIP effect (TWinnig Induced Plasticity) [11-13].

In contradistinction to numerous researches performed to determine the behaviour of high-manganese steels in the conditions of cold plastic deformation, not many works devote attention to hot plastic deformation of this group of steels. To develop the manufacturing methods, it is important to determine the flow behaviour of steels under hot working conditions. There is a shortage of sufficient information in science publications. In the work [14], the influence of initial grain size and deformation parameters on plasticity characteristics obtained in hot torsion tests for 18Cr-8Ni and 18Cr-17Mn-0.5C steels was investigated. It was found that Cr-Mn steel characterizes with much higher intensity of strain hardening than Cr-Ni steel, which makes more difficulties during plastic deformation. Higher intensity of strengthening of the steel with addition of manganese causes occurrence of maximal flow stress for smaller ϵ_{max} value. It gives opportunity for the refinement of structure by dynamic recrystallization. This phenomenon was investigated by Hamada

et. al. [15] in 25Mn and 25Mn3Al steels in a temperature range from 900 to 1100°C. It was found that maximal flow stress at a temperature of 1100°C for 25Mn steel occurs for $\epsilon_{\text{max}} = 0.17$.

Application of thermo-mechanical treatment consisting in immediate cooling of products from a finishing temperature of hot-working in controlled conditions should increase mechanical properties [16]. Thermo-mechanical treatment of Hadfield's steel was investigated by Król [17] where was found that dynamic recrystallization can occur after deformation with 30% reduction at a temperature of 800°C. Introduction of Nb and Ti microadditions to steels could be the reason for additional strain hardening of high-manganese steels and allows forming a fine-grained microstructure in successive hot-working stages [18]. These elements forming dispersive nitrides, carbonitrides and carbides, are the cause of additional precipitation strengthening what has a particular meaning for steels with austenitic matrix and relatively low yield stress.

2. Experimental procedure

Investigations were carried out on two high-manganese austenitic Mn-Si-Al steels containing Nb and Ti microadditions (Table 1). Melts were realized in the Balzers VSG-50 inductive vacuum furnace. Ingots with a mass of 25 kg were submitted open die forging on flats with a width of 220 mm and a thickness of 20 mm. Then, cylindrical samples $\varnothing 10 \times 12$ mm were made.

Table 1.
Chemical composition of the investigated steels

Mass contents, (%)							
C	Mn	Si	Al	P	S	Nb	Ti
Steel no. 1							
0.065	26.0	3.08	2.87	0.004	0.013	0.034	0.009
Steel no. 2							
0.040	27.5	4.18	1.96	0.002	0.017	0.033	0.009

Obtaining fine-grained austenite microstructure requires a proper selection of plastic working conditions adjusted to the precipitation kinetics of nitrides and carbides of microadditions introduced into the steel. Decisive meaning for impeding the grain growth of primary austenite in successive stages of hot-working should belong to TiN and NbC, which precipitation kinetics in austenite are described by kinetic Equations (1, 2). In order to determine the influence of MX-type interstitial phases on limiting the grain growth of steel, samples were solution heat-treated in water from a range of austenitizing temperature, from 900 to 1100°C.

$$\log [\text{Ti}] [\text{N}] = 0.32 - 8000/T \quad (1)$$

$$\log [\text{Nb}] [\text{C}] = 3.04 - 7290/T \quad (2)$$

where: [Ti], [Nb], [N], [C] – mass fractions of Ti and Nb as well as N and C dissolved in austenite at the T temperature (in K), the constants: A=8000, B=0.32 for TiN and A=7290, B=3.04 for NbC, given in [3] were used.

Determination of processes controlling strain hardening was carried out in continuous compression test using Gleeble 3800 thermo-mechanical simulator. In order to eliminate welding of sample with a die and decrease the friction on die – sample contact surface, very thin tantalum foil covered with lubricant based on nickel was introduced between the contact surfaces. The σ - ε curves were defined in a temperature range from 850 to 1050°C, for 10s^{-1} of strain rate. Identification of thermally activated processes controlling the course of strain hardening was performed through quenching of samples in water from the temperature of 950 and 850°C after applying true strain equal 0.29, 0.50 and 0.91. In order to determine the progress of recrystallization in the conditions simulating intervals between roll passes, part of samples was subjected to the heat treatment presented in Fig. 1. After true strain equal 0.29 in the temperature of 900°C, samples were isothermally held for up to 64s and then water-quenched for microstructure freezing.

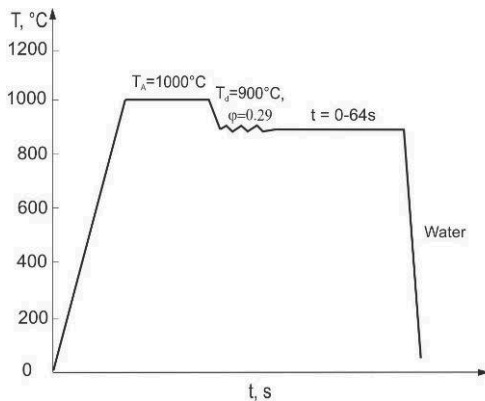


Fig. 1. Parameters of the thermo-mechanical processing aiming at determination of the recrystallization progress after plastic deformation at 900°C

Metallographic examinations of samples were carried out using the LEICA MEF4A light microscope. In order to reveal austenite structure, the samples etched in a mixture of nitrous and hydrochloric acid in various proportions. Identification of the phase composition of steels in the initial state and after thermo-mechanical treatment achieved using the X'Pert PRO diffractometer with X'Celerator detector. The lamp with Co anode was applied.

3. Results and discussion

Minor differences between chemical composition of elaborated steels result in slightly different microstructure in the initial state. Steel no. 1 is characterized by homogeneous microstructure of austenite with grain sizes equal approximately $80\mu\text{m}$, in which numerous annealing twins can be identified (Fig. 2b). Single-phase microstructure of the steel is confirmed by X-ray diffraction pattern in Fig. 2a. Increased concentration of silicon and decreased concentration of aluminium in steel no. 2 decides about the presence of certain portion of ε martensite apart

from annealing twins in microstructure. This phase is present in a form of parallel plates, not exceeding boundaries of specified grain (Fig. 3b). Its presence is confirmed by peaks shown in Fig. 3a. Thermodynamic calculations performed using Equations (1) and (2) allowed determining kinetics of TiN and NbC dissolution in the function of temperature. Taking into account atomic weights of Ti and N, the concentration of titanium necessary for binding the whole nitrogen into TiN is equal $3.4\%N = 0.0095\%$. This concentration corresponds with titanium concentration in both steels, what allows excluding formation of TiC and NbN, and the analyses can be simplified to examination of TiN and NbC. The beginning of TiN precipitation occurs at the temperature equal around 1350°C (Fig. 4a) what allows excluding formation of big particles, susceptible to coagulation [3]. Gradual decrease of participation of titanium dissolved in solid solution and increase of TiN participation occur along with decrease of temperature (Fig. 4b). Complete binding of Ti into TiN is present at the temperature of approximately 900°C. The beginning of niobium carbide participation in steel no. 1 occurs in the temperature of approximately 1010°C, and its finish - at temperature close to 800°C (Fig. 5). Due to lower carbon concentration in steel no. 2, temperature of the beginning of NbC precipitation decreases to around 970°C. In reality, apart from TiN and NbC precipitations, (Ti,Nb)(C,N)-type complex particles should be expected, particularly in a temperature range 1010-900°C, corresponding with the end of TiN precipitation and beginning of precipitation of NbC.

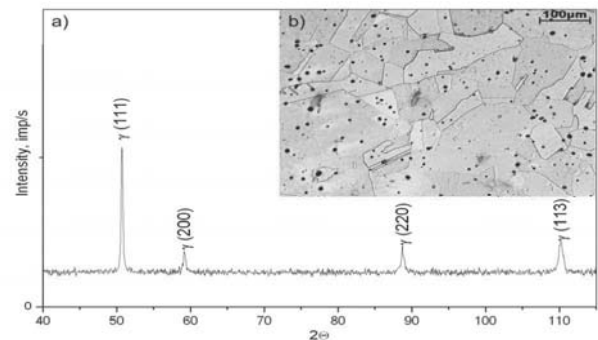


Fig. 2. X-ray diffraction pattern (a) and the structure of the 26Mn-3Si-3Al-Nb-Ti steel in the initial state (b)

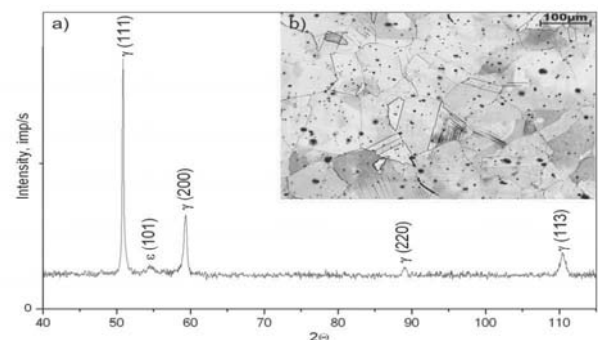


Fig. 3. X-ray diffraction pattern (a) and the structure of the 27Mn-4Si-2Al-Nb-Ti steel in the initial state (b)

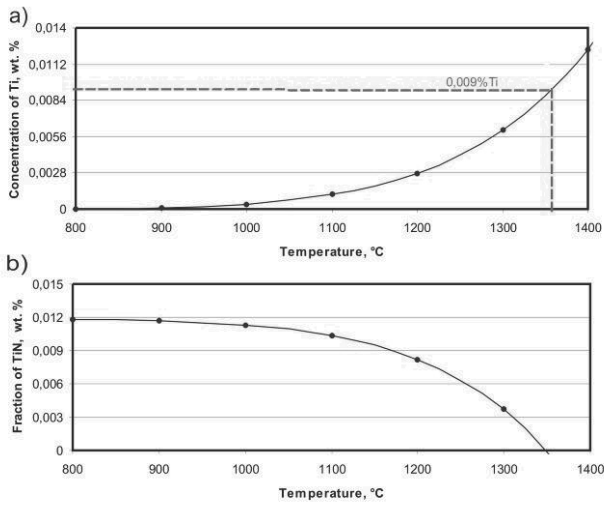


Fig. 4. Dissolution kinetics of TiN as a function of temperature; a) changes of Ti concentration, b) changes of TiN fraction; 26Mn-3Si-3Al-Nb-Ti steel

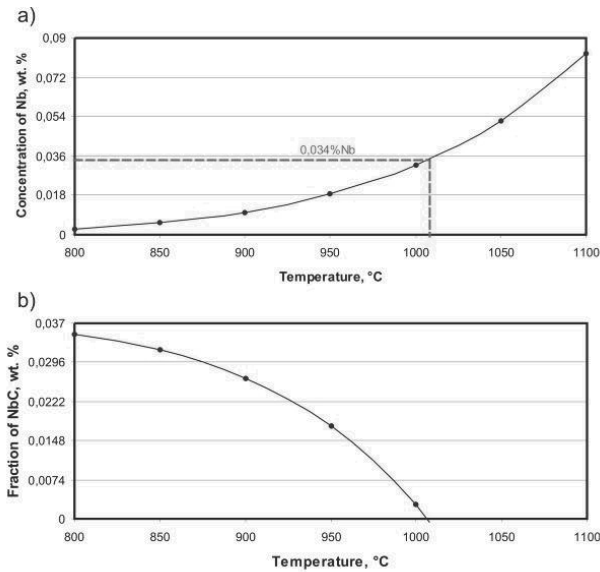


Fig. 5. Dissolution kinetics of NbC as a function of temperature; a) changes of Nb concentration, b) changes of NbC fraction; 26Mn-3Si-3Al-Nb-Ti steel

Advantageous influence of dispersive particles of MX-type interstitial phases on limitation of grain growth in both steels is presented in Fig. 6a. Up to temperature of 1000°C grain size of austenite doesn't exceed 24µm, and then intensively increases to around 50µm. Austenite microstructures of steel no. 2 for samples solution heat treated from temperature of 900 and 1000°C are shown in Fig. 6b and 6c. Together with increase of solution heat treatment temperature to 1100°C, grain size of γ phase increases vehemently (Fig. 6d). It should be connected to total dissolution

of NbC particles and gradual dissolution of TiN. Additionally, numerous annealing twins and laths of ϵ martensite can be observed in microstructure.

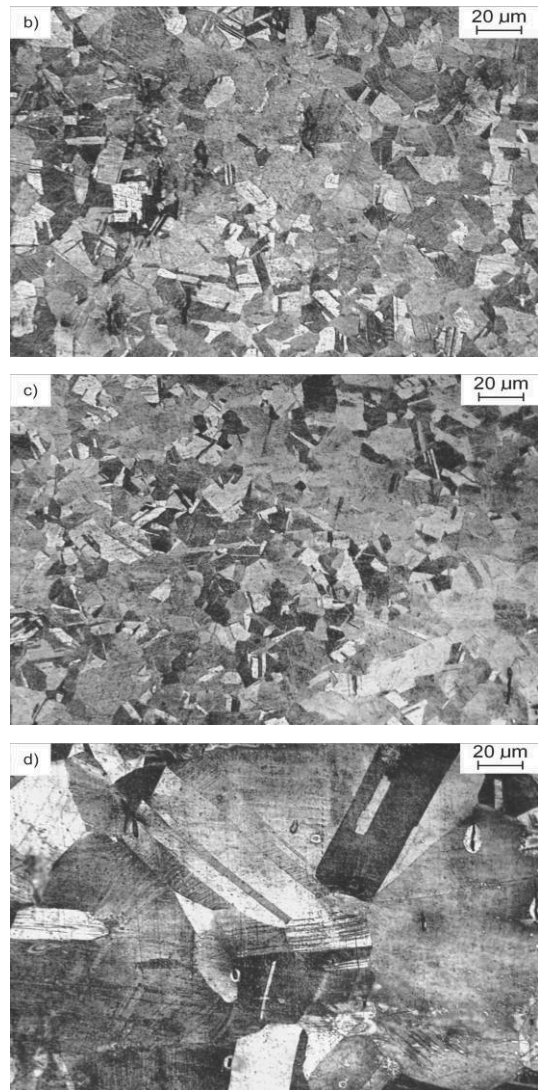
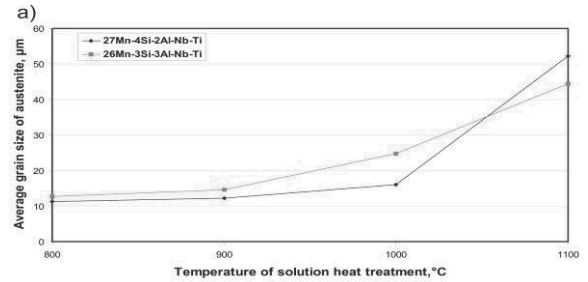


Fig. 6. Changes of austenite grain size as a function of temperature (a) and structures obtained after solution heat treatment from a temperature: b) 900°C, c) 1000°C, d) 1100°C; 27Mn-4Si-2Al-Nb-Ti steel

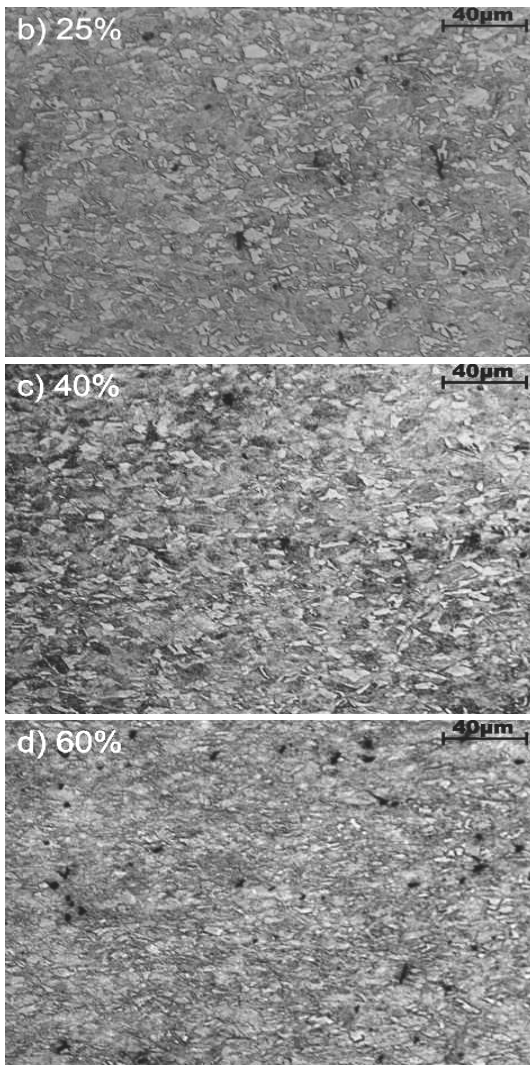
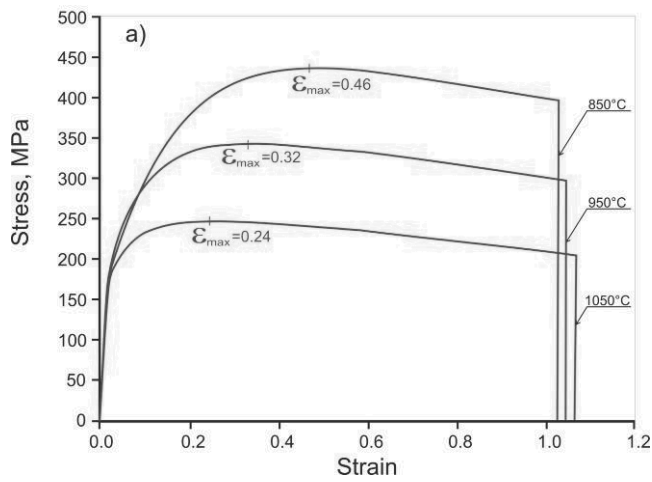


Fig. 7. Stress-strain curves of the 26Mn-3Si-3Al steel – (a), and austenitic structures of the specimen solution heat-treated from 850°C after deformation 20% (b), 40% (c) and 60% (d)

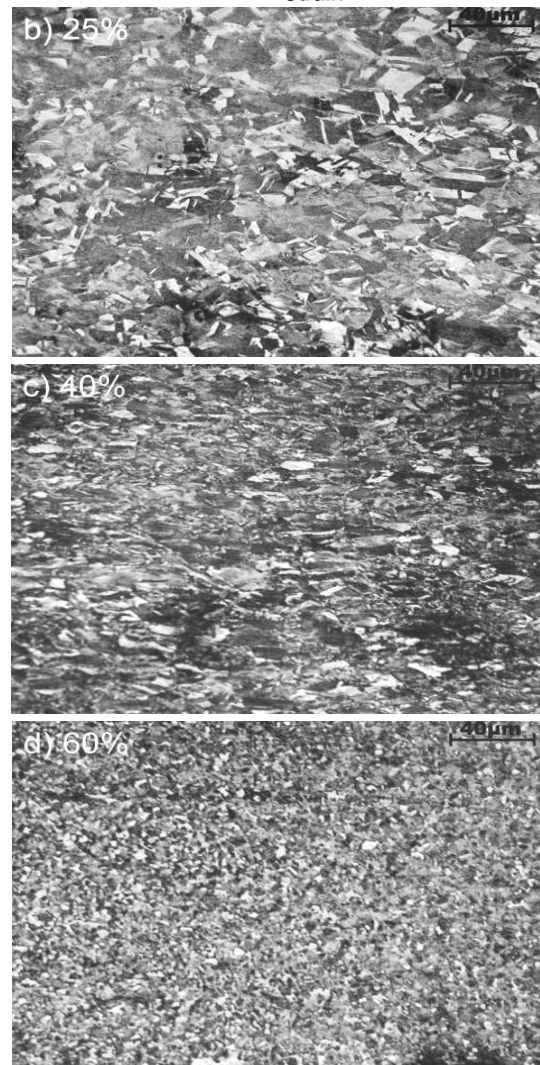
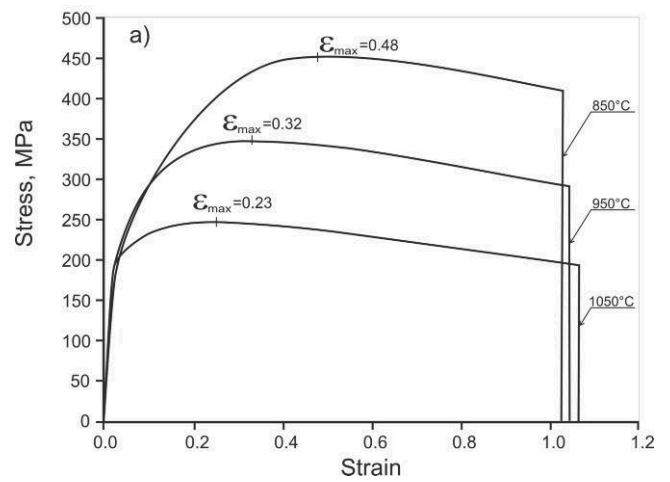


Fig. 8. Stress-strain curves of the 27Mn-4Si-2Al steel – (a), and austenitic structures of the specimens solution heat-treated from 850°C after deformation 20% (b), 40% (c) and 60% (d)

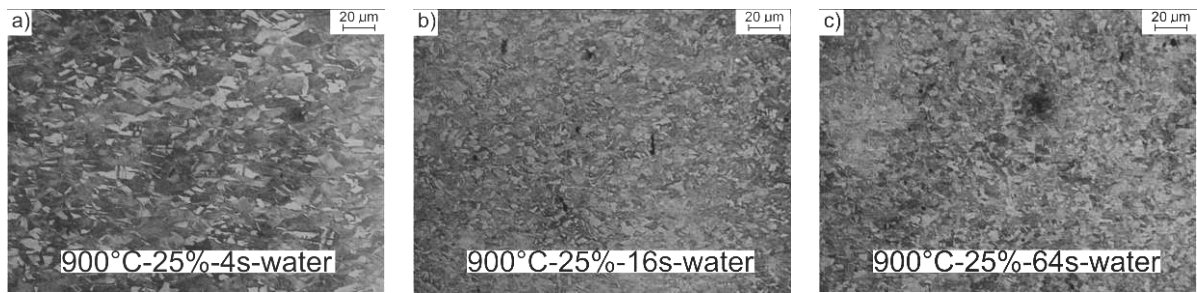


Fig. 9. Microstructure evolution of the 26Mn-3Si-3Al-Nb-Ti steel after isothermal holding for time: a) $t = 4\text{s}$; b) $t = 16\text{s}$; c) $t = 64\text{s}$; for the specimens plastically deformed at 900°C , $\varepsilon = 0.29$

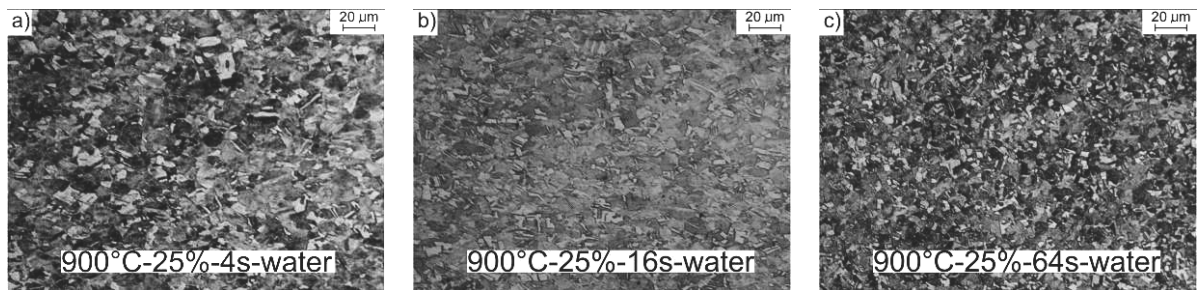


Fig. 10. Microstructure evolution of the 27Mn-4Si-2Al-Nb-Ti steel after isothermal holding for time: a) $t = 4\text{s}$; b) $t = 16\text{s}$; c) $t = 64\text{s}$; for the specimens plastically deformed at 900°C , $\varepsilon = 0.29$

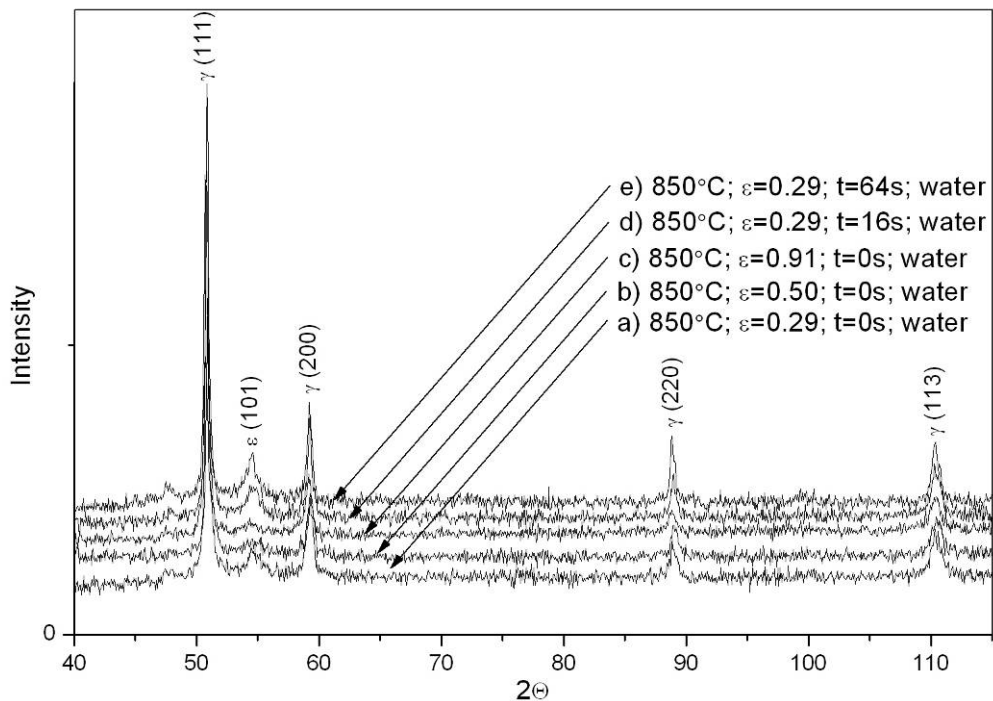


Fig. 11. X-ray diffraction patterns for 27Mn-4Si-2Al-Nb-Ti steel after various variants of the thermo-mechanical treatment; a) 850°C , $\varepsilon = 0.29$, $t = 0\text{s}$; b) 850°C , $\varepsilon = 0.5$, $t = 0\text{s}$; c) 850°C , $\varepsilon = 0.91$, $t = 0\text{s}$; d) 850°C , $\varepsilon = 0.29$, $t = 16\text{s}$; e) 850°C , $\varepsilon = 0.29$, $t = 64$

Continuous compression tests allowed determining the range of yield stress of produced steels in a temperature range from 1050°C to 850°C. It arises from Figs. 7a and 8a that yield stress is equal from 230 to 450MPa. These values are considerably higher than they are for conventional C-Mn steels [18] and for Cr-Ni and Cr-Mn austenitic steels [14]. Increase of yield stress along with decrease of compression temperature is accompanied by translation of ϵ_{\max} deformation in the direction of higher strains. High values of yield stress come from hardening influence of high concentration of Mn, Si and Al, as well as Nb and Ti microadditions in investigated steels. At 850°C steel no. 1 has slightly lower values of flow stress when comparing to steel no. 2. It's probably connected with lower concentration of silicon in steel no. 1. Microstructures of steel no. 1 set up in Fig. 7b-d are helpful in determining mechanisms controlling the course of strain hardening in the temperature of 850°C. It arises from Fig. 7b that the initiation of dynamic recrystallization occurs already after true deformation equal 0.29 (engineering deformation: 25%). It's admittedly lower than ϵ_{\max} , however, according to [20], dynamic recrystallization can be initiated already at critical deformation $\epsilon_{\text{cd}}=(0.5-0.85)\epsilon_{\text{m}}$. Apart from large grains, fine dynamically recrystallized grains are also visible. Participation of fine grains arranged in matrix of dynamically recovered grains essentially increases after increasing true strain to 0.5 (Fig. 7c). Fully dynamically recrystallized microstructure of steel can be obtained after true deformation equal 0.9 (Fig. 7d). Limiting deformation leading to dynamic recrystallization of steel no. 2 is also equal 0.29 (Fig. 8b) and participation of recrystallized grains increases along with increase of degree of deformation (Fig. 8c). After true strain equal 0.9 even more fine-grained microstructure of dynamically recrystallized grains was achieved, in comparison with steel no. 1 (Fig. 8c).

Development of microstructure of steel no. 1 isothermally held in temperature of 900°C, after true strain equal 0.29 is presented in Fig. 9. After 4s of holding, microstructure is slightly different in comparison with microstructure of steel solution heat treated directly after deformation (Fig. 9a). Increase of holding time to 16s results in obtaining high participation of recrystallized grains at the cost of dynamically recovered grains (Fig. 9b). Fast progress of microstructure reconstruction confirms occurrence of metadynamic recrystallization, not requiring any period of incubation. Confirmation of this fact is large portion of dynamically recrystallized grains after deformation with reduction of 25% at temperature of 850°C (Fig. 7b). Increase of holding time to 64s leads to achievement of highly fine-grained microstructure of metadynamically and statically recrystallized grains (Fig. 9c). Successive stages of microstructure development of steel no. 2 in function of isothermal holding time are shown in Fig. 10a-c. The progress of recrystallization of this steel is slightly slower, what proves higher contribution of static recrystallization to removal of strain hardening than in case of steel no. 1.

The conditions of hot-working additionally influence phase state of steel. Steel no. 1 with initial austenitic microstructure keeps its stability independently from conditions of plastic deformation. X-ray diffraction patterns for steel no. 2 indicate presence of peaks coming from ϵ martensite. However, their intensity connected with participation of this phase differs depending on applied variant of hot-working. The highest intensity from (100) and (101) planes belongs to the sample deformed with lowest reduction (Fig. 11a).

Increase of reduction causes decrease of peaks intensity (Fig. 11b, 11c). Isothermal holding for 16s after deformation at 900°C doesn't change phase composition of steel no. 2. Still, slight peaks coming from ϵ martensite are present (Fig. 11d). Increase of holding time to 64s leads to substantial increase of (100) and (101) peaks intensity of ϵ martensite (Fig. 11e). It means, that in spite of fine-grained microstructure of steel having impeding impact on growth of ϵ martensite laths [21], also state of internal stresses, effectively limited in process of metadynamic and static recrystallization, decides about tendency of formation of this phase in high-manganese steels.

4. Conclusions

Despite slight difference in chemical composition, brought mainly to concentration of Si and Al, elaborated steels show different microstructure in the initial state. Steel with higher Al concentration has stable microstructure of austenite with annealing twins, while steel with higher Si concentration consists of certain portion of ϵ martensite in form of plates. The differences in chemical composition don't have meaningful influence on behaviour of these steels in conditions of hot-working. Values of yield stress are equal from 230 to 450MPa, and values of ϵ_{\max} deformation come from a range from 0.23 to 0.48. Despite high value of ϵ_{\max} at temperature of 850°C, initiation of dynamic recrystallization occurs already after true strain equal approximately 0.29, what creates possibility of refinement of microstructure. Dynamic recrystallization occurs more intensively in the steel containing 3%Al and 3%Si. It also results in faster course of removing the effects of hardening in the consequence of metadynamic recrystallization during isothermal holding of this steel in temperature of 900°C. Removal of strain hardening effects in steel no. 2 takes place mainly with participation of static recrystallization. The conditions of hot-working additionally influence phase state of investigated steels. Steel no. 1 keeps stable austenite microstructure independently from conditions of plastic deformation. Steel with initial bi-phase microstructure keeps a certain portion of martensite, yet dependant on conditions of hot-working. Grain size of γ phase as well as the state of internal stresses dependent on thermally activated mechanisms removing effects of strain hardening, have decisive influence on precipitation of the phase.

Acknowledgements

Scientific work was financed from the science funds in a period of 2006-2008 in the framework of project No. 3 T08A 080 30.

References

- [1] A.D. Paepe, J.C. Herman, Improved deep drawability of IF-steels by the ferrite rolling practice, Proceedings of the 37th Mechanical Working and Steel Processing Conference, Baltimore, 1999, 951-962.

- [2] H. Takechi, Application of IF based sheet steels in Japan, Proceedings of the International Conference on the Processing, Microstructure and Properties of IF Steels, Pittsburgh, 2000, 1-12.
- [3] J. Adamczyk, Development of the microalloyed constructional steels, Journal of Achievements in Materials and Manufacturing Engineering 14 (2006) 9-20.
- [4] J. Adamczyk, A. Grajcar, Heat treatment and mechanical properties of low-carbon steel with dual-phase microstructure, Journal of Achievements in Materials and Manufacturing Engineering 22 (2007) 13-20.
- [5] A. Grajcar, Hot-working in the $\gamma+\alpha$ region of TRIP-aided microalloyed steel, Archives of Materials Science and Engineering 28 (2007) 743-750.
- [6] S. Ganesh Sundara Raman, K.A. Padmanabhan, Tensile deformation-induced martensitic transformation in AISI 304LN austenitic stainless steel, Journal of Materials Science Letters 13 (1994) 389-392.
- [7] G. Frommeyer, O. Grässel, High strength TRIP/TWIP and superplastic steels: development, properties, application, La Revue de Metallurgie-CIT 10 (1998) 1299-1310.
- [8] G. Frommeyer, U. Brüx, P. Neumann, Supra-ductile and high-strength manganese-TRIP/TWIP steels for high energy absorption purposes, ISIJ International 43 (2003) 438-446.
- [9] S. Allain, J.P. Chateau, O. Bouaziz, S. Migot, N. Guelton, Correlations between the calculated stacking fault energy and the plasticity mechanisms in Fe-Mn-C alloys, Materials Science and Engineering A 387-389 (2004) 158-162.
- [10] O. Grässel, L. Krüger, G. Frommeyer, L.W. Meyer, High strength Fe-Mn-(Al, Si) TRIP/TWIP steels development – properties – application, International Journal of Plasticity 16 (2000) 1391-1409.
- [11] S. Vercammen, B. Blanpain, B.C. De Cooman, P. Wollants, Mechanical behaviour of an austenitic Fe-30Mn-3Al-3Si and the importance of deformation twinning, Acta Materialia 52 (2004) 2005-2012.
- [12] A.K. Lis, B. Gajda, Modelling of the DP and TRIP microstructure in the CMnAlSi automotive steel, Journal of Achievements in Materials and Manufacturing Engineering 15 (2006) 127-134.
- [13] T. Bator, Z. Muskalski, S. Wiewiórkowska, J.W. Pilarczyk, Influence of the heat treatment on the mechanical properties and structure of TWIP steel in wires, Archives of Materials Science and Engineering 28/6 (2007) 337-340.
- [14] G. Niewielski, M. Hetmańczyk, D. Kuc, Influence of the initial structure and deformation conditions on properties of hot-deformed austenitic steels, Materials Engineering 24 (2003) 795-798 (in Polish).
- [15] A.S. Hamada, L.P. Karjalainen, M.C. Somani, The influence of aluminium on hot deformation behaviour and tensile properties of high-Mn TWIP steels, Materials Science and Engineering A 467 (2007) 114-124.
- [16] L.A. Dobrzański, A. Grajcar, W. Borek, Influence of hot-working conditions on a structure of high-manganese austenitic steels, Journal of Achievements in Materials and Manufacturing Engineering 29 (2008) 139-142.
- [17] S. Król, Influence of the thermo-mechanical processing and ageing on the structure and mechanical properties of the 11G12 Hadfield steel, PhD thesis, Silesian University of Technology, Gliwice, 1974.
- [18] J. Adamczyk, A. Grajcar, Structure and mechanical properties of DP-type and TRIP-type sheets, Journal of Materials Processing Technology 162-163 (2005) 267-274.
- [19] A. Grajcar, Effect of hot-working in the $\gamma+\alpha$ range on a retained austenite fraction in TRIP-aided steel, Journal of Achievements in Materials and Manufacturing Engineering 22 (2007) 79-82.
- [20] J. Adamczyk, Theoretical physical metallurgy, The Silesian University of Technology Publishers, Gliwice, 2002, (in Polish).
- [21] K.K. Jee, J.H. Han, W.Y. Jang, Measurement of volume fraction of ϵ martensite in Fe-Mn based alloys, Materials Science and Engineering A 378 (2004) 319-322.